Production of J/ψ-meson pairs and $4c$-tetraquark at LHC

A. V. Berezhnoy,[1, *] A. K. Likhoded,[2, †] A. V. Luchinsky,[2, ‡] and A. A. Novoselov[2, 3, §]

[1]*SINP of Moscow State University, Moscow, Russia*

[2]*Institute for High Energy Physics, Protvino, Russia*

[3]*Moscow Institute of Physics and Technology, Dolgoprudny, Russia*

Theoretical predictions for $pp \to 2J/\psi + X$ cross section at $\sqrt{s} = 7$ TeV with different kinematical restrictions are presented. Results are compared with the the first LHCb data available. Special attention is payed to possible signal from novel particles — tetraquarks build from two valence c-quarks and two valence $\bar{c}$-quarks. According to our estimates it is quite possible to observe at least one of these states (tensor tetraquark) experimentally under LHCb conditions.

PACS numbers: 13.85.Fb, 14.40.Rt

I. INTRODUCTION

Simultaneous production of two J/ψ-mesons was first observed in 1982 by the NA3 collaboration in multi-muon events in pion-platinum interactions at 150 and 280 GeV [1] and later at 400 GeV in proton-platinum collisions [2]. Cross-section of this reaction is suppressed compared to the single J/ψ production by more than three orders of magnitude, because of both higher order of perturbative QCD $O\left(\alpha_s^4\right)$ and kinematical reasons due to production of bigger mass. At NA3 energies main contribution to the cross section arose from quark-antiquark annihilation channel [3]. On the contrary, it is the $gg \to J/\psi J/\psi$ process studied in [4] which dominates at the LHC. Both contributions lead to the cross-section decreasing as the power of the invariant mass of the J/ψ pair ($\hat{\sigma} \sim 1/\hat{s}^3$ for the $q\bar{q}$-annihilation and $\hat{\sigma} \sim 1/\hat{s}^2$ for the gluonic production). It is worth mentioning that such decrease is absent in higher orders of perturbation theory and the cross-section of the $gg \to 2J/\psi + X$ process becomes constant at large invariant masses [5]. In current work we will be mainly interested in the low invariant mass region as it is most accessible in the LHCb experiment, which specializes in heavy quarks studies.

* Alexander.Berezhnoy@cern.ch

† Anatolii.Likhoded@ihep.ru

‡ Alexey.Luchinsky@ihep.ru

§ Alexey.Novoselov@cern.ch

In the leading order in α_s quarkonia pair production process obeys selection rules similar to those in quarkonia decays. Two initial gluons in a color-singlet state are C-even. That is why production of J/ψ-, η_c- or χ_c-meson pairs is allowed while combined production of 2 particles having different C-parity (such as $J/\psi + \eta_c$ and $J/\psi + \chi_c$) is prohibited.

First comparison of the NA3 data with QCD predictions has shown 2 times shortage of the prediction [3]. Taking additional contribution from the P-wave state χ_c or ψ'-meson decay to J/ψ into account could improve the agreement. Selection rules mentioned above put restrictions on the feed down from the higher states. For instance feed down from the $J/\psi + \chi_c$ production is expected to be less than from the $\chi_c + \chi_c$ one as production of the former final state is prohibited in leading order. Meanwhile feed down from the $J/\psi + \psi'$ channel is expected to be quite large. In principle, other mechanisms of J/ψ-pair production are possible at the same order in α_s. First of all it is contribution of the color-octet states which plays significant role in the single J/ψ production in the high-p_T region. Cross section of the color-octet states production falls more slowly as transverse momenta grows than that of the color-singlet one. However at small transverse momenta and small invariant masses of the J/ψ pair smallness of the color-octet matrix element in the wave function of the J/ψ meson compared to the color-singlet one obviously leads to the negligible contribution. As shown in [6, 7] octet contribution becomes significant only at transverse momentum $p_T \gtrsim 15$ GeV (which corresponds to big invariant mass of the J/ψ pair). Another possibility to enlarge theoretical prediction is connected with the rearrangement of c-quarks in the final state, when instead of two colorless $c\bar{c}$-pairs two diquarks, cc and $\bar{c}\bar{c}$, are produced. After interaction in the final state they can form a pair of double-heavy baryons above the threshold of their production or a pair of J/ψ-mesons below it.

The region of small invariant masses of the J/ψ-pair is most interesting due to the opportunity for two diquarks $[cc]_{\bar{3}_c} + [\bar{c}\bar{c}]_{3_c}$ to form a bound state — tetraquark, which decays to a J/ψ-pair. Attraction between $\bar{3}_c$- and 3_c-states does not exclude such a possibility, especially since similar exotic states like $Y(3940)$ resonance decaying to $J/\psi\omega$ [8] and $Y(4140)$ resonance decaying to $J/\psi\phi$ [10, 11] have recently been observed.

In addition, pair production of J/ψ-mesons has been earlier discussed as a possible way to observe C-even states of bottomonia. Production of scalar and tensor χ_b-mesons was considered in [12, 13], production of an η_b-meson — in [14].

The second section of our article is devoted to the non-resonant production of J/ψ-
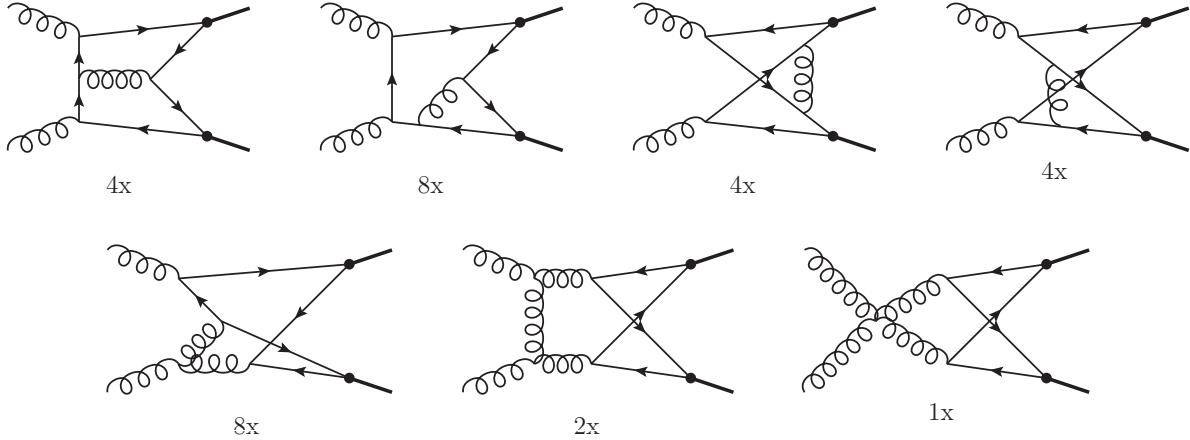
FIG. 1. Feynman diagrams contributing $gg \to 2J/\psi$ process.

meson pairs in the gluon-gluon interaction. In the third section cross section of this process at LHC at 7 TeV energy is calculated taking different experimental restrictions into account. Special attention is payed to production in LHCb conditions as there is first experimental data available [15]. Fourth section is devoted to calculation of the $4c$-tetraquark mass and estimation of the cross section of its production at LHC.

II.   DOUBLE J/ψ-MESON PRODUCTION IN GLUON-GLUON INTERACTION

In the leading order of perturbative QCD there are 31 Feynman diagrams describing color-singlet charmonium pairs production in gluonic reaction (see fig.1). We are not considering contribution of the quark-antiquark interaction, which is negligibly small at LHC energies. Hadronization of a $c\bar{c}$-pair into a final J/ψ-meson is accounted for by the wave function of this particle at origin:

$$\psi_{J/\psi}(r)\big|_{r=0} = 0.21\,\mathrm{GeV}^{3/2}. \tag{1}$$

It is the only nonperturbative parameter in the matrix element of $gg \to 2J/\psi$ process. Its value is extracted from the leptonic width of J/ψ-meson neglecting QCD corrections as we do not take these corrections into account in our matrix element. Color-octet contributions in the kinematical region considered in our article can be neglected [6, 7].

In the following we will use two methods to calculate the cross section. First approach involves standard procedure of analytical calculation of the amplitude, analytical squaring of this amplitude (for example, using FeynCalc package [16]) and subsequent integration

TABLE I. Cross section of $gg \to 2J/\psi$ processes for different combinations of final particle's polarizations

$\sqrt{\hat{s}}$, GeV	$\hat{\sigma}(LL)$, pb	$\hat{\sigma}(LT)$, pb	$\hat{\sigma}(TT)$, pb
6.2	1.59	4.66	5.75
6.5	1.75	5.04	6.69
7.0	1.47	3.99	5.96
8.0	0.86	2.03	3.75
9.0	0.50	1.09	2.26
10.0	0.30	0.59	1.39
12.0	0.11	0.196	0.57
14.0	0.046	0.074	0.26
16.0	0.022	0.031	0.136
18.0	0.011	0.014	0.071
20.0	0.006	0.0071	0.043

over the phase space. Second method which we use is based on numerical calculation of the amplitude at each point of the phase space, followed by squaring (see papers [17, 18] for more details). The latter method is associated with a smaller number of analytical calculations and makes it easier to consider different quantum numbers of the final particles and their polarizations. Comparison of results obtained by these two methods also help to check correctness of the calculations. Both methods give values that agree with each other and coincide within errors of calculations with results presented in [4, 19].

In fig.2 the cross section of double J/ψ-meson production in gluonic interaction versus invariant mass of the pair is shown for different combinations of polarizations. Table I shows cross section of the J/ψ pair production for various polarizations of each of J/ψ-particles. It can be seen that near the threshold cross sections of transversely and longitudinally polarized J/ψ-meson production are comparable, while at higher p_T (and hence large invariant mass of the gluon pair), J/ψ-mesons are mainly transversely polarized (see also [6, 7]). As an example, in fig.3 we show angular distribution of polarized J/ψ-mesons, produced in $gg \to 2J/\psi$ reaction at $\sqrt{\hat{s}} = 10$ GeV. One can easily see, that angular distributions for different combinations of polarizations differ drastically.
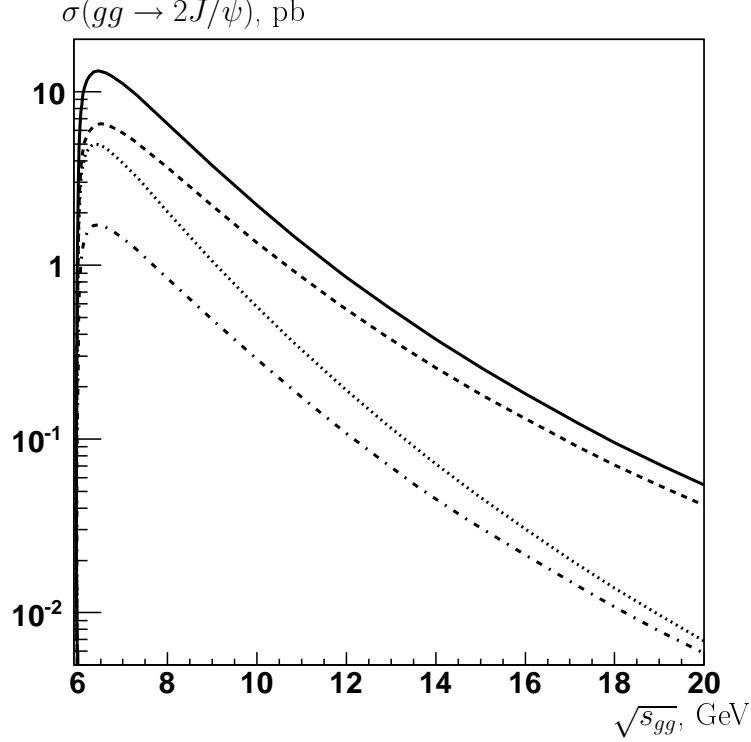
FIG. 2. Cross section of double J/ψ-meson gluonic production as a function of their invariant mass: solid curve — total cross section; dashed curve — both mesons are transversely polarized; dotted curve — one meson is transversely polarized, another — longitudinally; dash-dotted curve — both mesons are longitudinally polarized.

Partonic cross-section summed over polarizations as a function of $\hat{s}$ is equal

$$\hat{\sigma}(\hat{s}) = \frac{512\pi^3\psi(0)^4\alpha_s^4}{1215m^4\hat{s}^7} \times \tag{2}$$

$$\times \left(\hat{s}(5\hat{s}^4 + 874m^2\hat{s}^3 + 13368m^4\hat{s}^2 + 36594m^6\hat{s} + 90m^8)\sqrt{1 - \frac{4m^2}{\hat{s}}} + \right.$$

$$\left. + 30m^4(6m^6 + 70m^4\hat{s} - 1025m^2\hat{s}^2 - 134\hat{s}^3)\log\frac{1 + \sqrt{1 - \frac{4m^2}{\hat{s}}}}{1 - \sqrt{1 - \frac{4m^2}{\hat{s}}}} \right)$$

Near the threshold there is a typical square-root dependence ($\hat{\sigma} \sim \sqrt{\hat{s} - 4m_{J/\psi}^2}$), which corresponds to the production of a pair in S-wave state. At large invariant masses expression (2) tends to $\sim \hat{s}^{-2}$ asymptotics.

As noted in the introduction J/ψ- and ψ'-meson or pair of ψ'-mesons can be produced by the same mechanism in gluon-gluon interactions. According to dimensional considerations, ratios of yields of different meson pairs are determined by the ratios of their wave functions
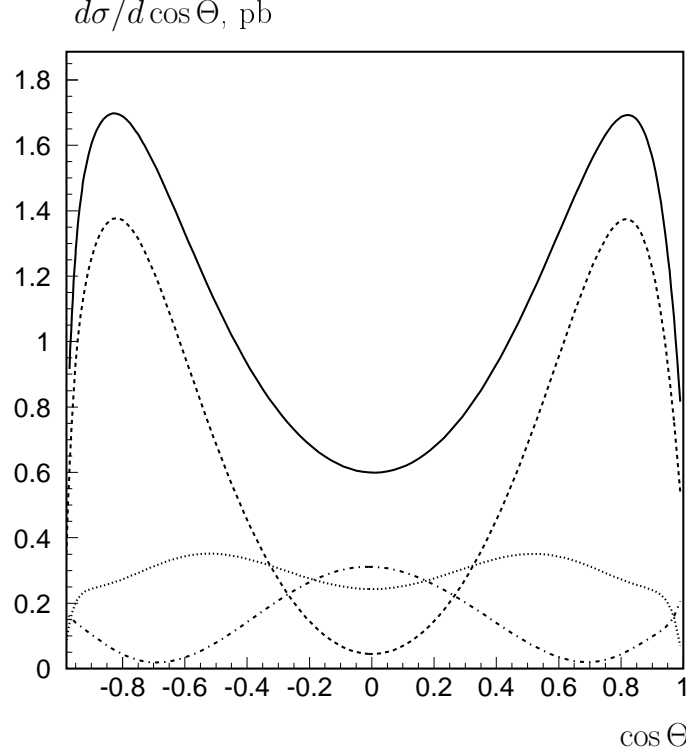
FIG. 3. Angular distribution of different polarization states in $gg \rightarrow 2J/\psi$ reaction at $\sqrt{\hat{s}} = 10$ GeV: solid curve — total cross section; dashed curve — both mesons are transversely polarized; dotted curve — one meson is transversely polarized, another — longitudinally; dash-dotted curve — both mesons are longitudinally polarized.

at origin and masses:

$$\sigma(2J/\psi) : \sigma(J/\psi + \psi') : \sigma(2\psi') \sim \frac{\psi_{J/\psi}^4(0)}{m_{J/\psi}^8} : \frac{2\psi_{J/\psi}^2(0)\psi_{\psi'}^2(0)}{((m_{J/\psi} + m_{\psi'})/2)^8} : \frac{\psi_{\psi'}^4(0)}{m_{\psi'}^8}. \tag{3}$$

The yield of non-identical particles is factor 2 enhanced compared to the yield of identical ones. We estimate contribution of the $gg \rightarrow J/\psi\psi'$ process by substituting $(m(J/\psi) + m(\psi'))/2$ for $m(J/\psi)$ in the matrix element and using the appropriate $\psi(0)$ for the second quarkonium. For ψ' this value determined from the leptonic width is equal

$$\psi_{\psi'}(r)|_{r=0} = 0.16 \, \text{GeV}^{3/2}. \tag{4}$$

Taking numerical values into account one gets approximately

$$\sigma(2J/\psi) : \sigma(J/\psi + \psi') : \sigma(2\psi') \sim 1 : 1/2 : 1/12. \tag{5}$$

Noticing that branching fraction of $\psi' \rightarrow J/\psi + X$ decay is about 56% one concludes that feed down from this excited state is nearly 30%.

Determination of feed down from P-wave states like χ_c requires calculation of another matrix element with 2 P-wave particles in the final state. Meanwhile production of $\chi_c + J/\psi$ states is suppressed by C-parity conservation and feed down from χ_c pairs is suppressed by branching squared. Naive estimation of feed down from the latter process leads to the value of about 6% in low invariant mass region.

As noted above, near the threshold one of the sources of J/ψ-pair is gluonic production of cc and $\bar{c}\bar{c}$ diquarks. This reaction is described by the diagrams similar to those shown in fig.1, but with changed color factors and value of wave function at origin. The last parameter can be calculated in the framework of potential model. According to paper [20] its numerical value is equal

$$\psi_{[cc]}(r)\big|_{r=0} = 0.15 \, \text{GeV}^{3/2}. \tag{6}$$

In fig.4 the cross section of double diquark production in gluonic interaction as a function of its invariant mass is shown. Below the threshold of two Ξ_{cc}-baryons production at $m_{gg} \approx 7$ GeV we expect the transition of this state into a pair of J/ψ-mesons or a tetraquark, that can be observed as a peak in the $J/\psi J/\psi$ mass spectrum.

III. PRODUCTION AT LHC

To calculate the cross section of charmonia pairs production in hadronic experiments one needs to convolute partonic cross section presented in the previous section with the distribution functions of partons in the initial hadrons:

$$d\sigma\left(pp \to 2J/\psi + X\right) = \int dx_1 dx_2 f_i\left(x_1\right) f_j\left(x_2\right) d\sigma(ij \to 2J/\psi), \tag{7}$$

where $x_{1,2}$ are the momentum fractions carried by partons. As already mentioned, gluon interaction gives main contribution at the LHC energies, so it is sufficient to take only gluon fusion into account. Typical values of x are small, $x_{1,2} \sim 10^{-3}$. According to our calculations total cross section of the direct J/ψ pairs production in proton-proton interaction at $\sqrt{s} = 7$ TeV is equal to

$$\sigma\left(pp \to 2J/\psi + X\right) = 18\,\text{nb},$$

This value agrees well with previous results ([6], for example). Leading order expression for the running strong coupling constant $\alpha_s(\hat{m}_T)$ was used to obtain this value. It is clear that
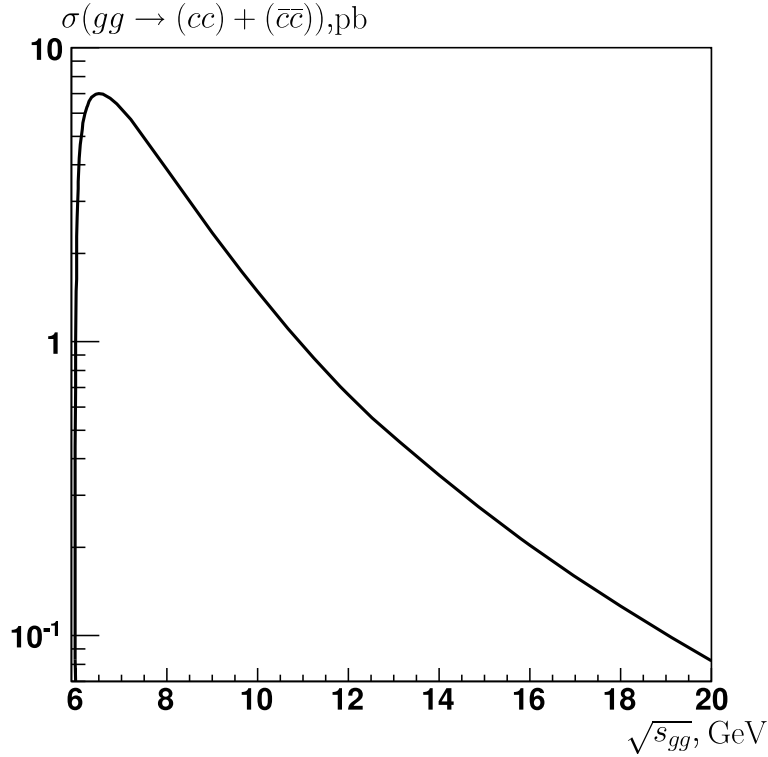
FIG. 4. Cross section of diquark-antidiquark gluonic production as a function of their invariant mass.

since the cross section of the $gg \to 2J/\psi$ process is proportional to α_s^4, final result depends strongly on the choice of this constant. For gluon PDFs CTEQ5L [22] parametrization at $\hat{m}_T$ scale was used as the most natural one for the leading order QCD process.

It worth mentioning that simple expression (7) does not account for the transverse momentum of gluons induced by the radiation in the initial state (ISR). This effect obviously does not affect value of the total cross section, but may be significant for the transverse momentum distribution of the final particles as well as for the cross sections in different detectors. In our work ISR is taken into account by the Pythia 6.4 MC generator [21]. Standard tune of the version 6.4.25 was used.

To obtain predictions for specific experiment it is necessary take kinematical constraints imposed by the detector into account. For instance, at the LHCb experiment main limitation is imposed on the rapidity of the final charmonium: $2 < y < 4.5$, while there is virtually no cutoff on the transverse momentum. Fig. 5 shows rapidity distribution of the J/ψ-meson at the $\sqrt{s} = 7$ TeV energy. Solid and dashed lines correspond to the transverse motion of partons accounted for and neglected, respectively. Cross section of the J/ψ pair production
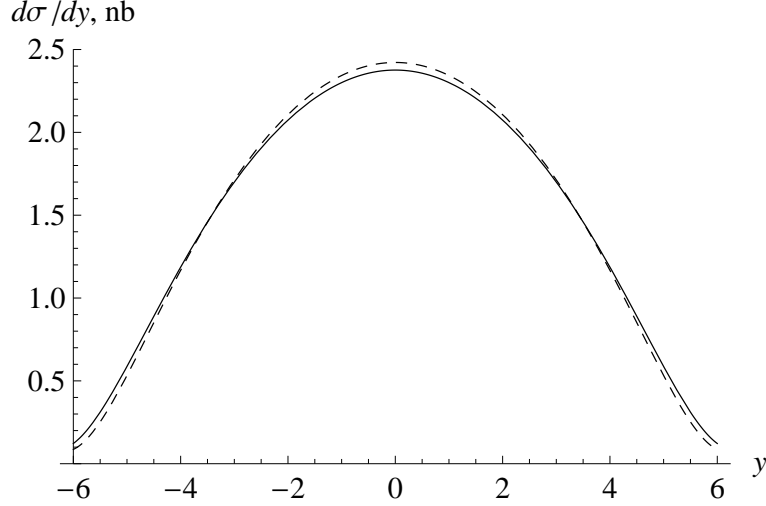
FIG. 5. Rapidity distribution of the final charmonium in the reaction $pp \to 2J/\psi + X$. Solid and dashed lines show the results obtained with the initial state radiation accounted for and in the collinear approximation, respectively.

with the $2 < y < 4.5$ restriction imposed is equal

$$\sigma^{coll.}_{\text{LHCb}} (pp \to 2J/\psi + X) = 3.2 \, \text{nb}$$

if the initial state radiation is neglected, and

$$\sigma_{\text{LHCb}} (pp \to 2J/\psi + X) = 3.1 \, \text{nb}$$

if accounted for. One can see that refusal from the collinear approximation affects cross section of the double J/ψ production in LHCb very slightly. This guaranties that uncertainty induced by the ISR effect on the fraction of total cross section selected by the cutoff is small compared to uncertainty in value of the total cross section itself. The latter dues to α_s, $\psi_{J/\psi}(0)$ and m_c values and reaches 30%.

The case is completely different for the detectors examining central region and limiting minimal transverse momentum (such as ATLAS and CMS). The restrictions on the transverse momentum and rapidity of the final charmonia are:

$$p_T > 5 \, \text{GeV}, \quad |y| < 2.5.$$

Fig. 6 shows distributions over the transverse momentum of one of the J/ψ-mesons obtained in the collinear approximation and taking the ISR into account. It can be seen that accounting for the ISR leads to a substantial broadening of the transverse momentum distribution
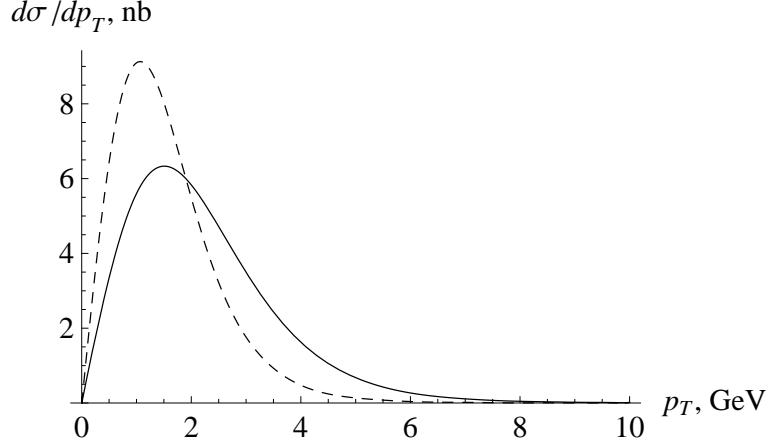
FIG. 6. Transverse momentum distribution of the single J/ψ-meson obtained with the initial state radiation accounted for (solid line) and in the collinear approximation (dashed line).

as compared to the collinear approximation. According to our calculations cross section of the J/ψ pair production in the collinear approximation taking the ATLAS cutoffs into account equals

$$\sigma_{\text{ATLAS}}^{collinear}\,(pp \to 2J/\psi + X) = 0.09\,\text{nb},$$

while accounting for the transverse motion of gluons lead (with the same cutoffs) to the value

$$\sigma_{\text{ATLAS}}\,(pp \to 2J/\psi + X) = 0.06\,\text{nb}.$$

Opposite to the situation in LHCb, this value is very model-dependent. Moderate ISR decreases fraction of events selected by the cutoff, as for two particles with transverse momenta slightly above the cutoff it often moves one of them below the cutoff value. Intensive ISR can increase this fraction as momenta of initial gluons more often become compatible with the cutoff value and more particles exceed the cutoff. Meanwhile behavior of the gluon's distribution over p_T in the high p_T region is worst known. Values of the cross section under ATLAS conditions can differ in several times depending on the tune of Pythia used.

To demonstrate importance of the initial state radiation we present the p_T-distribution of the J/ψ-pair (fig.7). In the collinear approximation this distribution is obviously described by the δ-function.

Solid curve in fig. 8 shows distribution over the invariant mass of the J/ψ pair. One can see that without cutoff in transverse momentum main part of events is concentrated in the
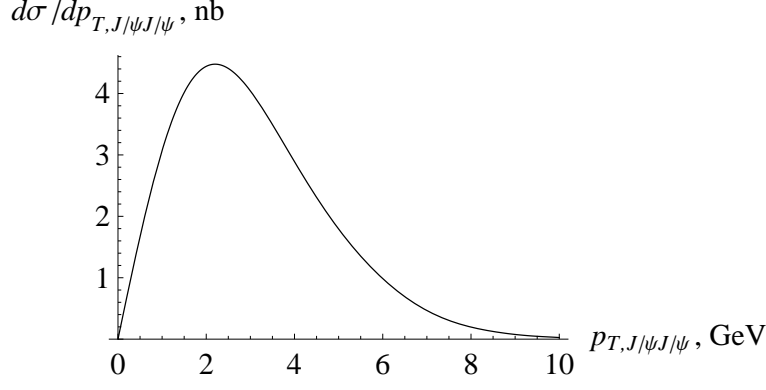
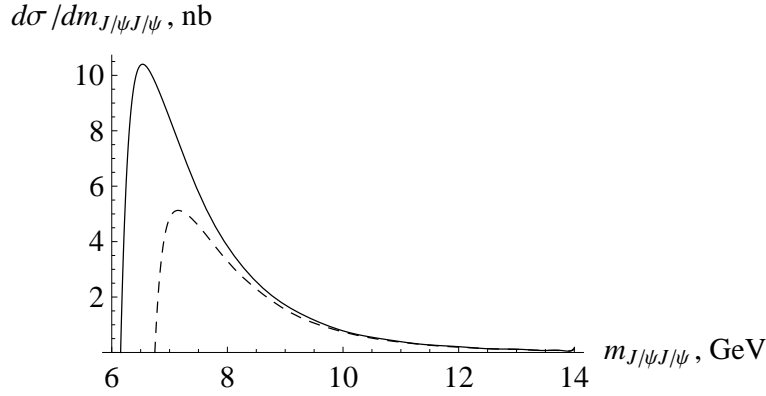FIG. 7. Distribution over the transverse momentum of the J/ψ pair.

FIG. 8. Distribution over the invariant mass of charmonium pairs in the $pp \to J/\psi + X$ (solid curve) and $pp \to J/\psi + \psi'$ (dashed curve) reaction.

low invariant mass region. Taking the transverse motion of the gluons into account virtually does not affect shape of the invariant mass distribution, as expected. Dashed curve in fig. 8 corresponds to the production of the $J/\psi + \psi'$ final state. This distribution obviously starts at bigger invariant mass value than those of the J/ψ-pair. Meanwhile invariant masses of J/ψ-pairs in which one of J/ψ-mesons originate from the ψ' decay ($\psi' \to J/\psi\pi\pi$ mostly) are distributed similarly to direct J/ψ-pairs. Both distributions and their total are presented in fig. 9. Kinematical cutoff corresponding the LHCb detector ($2 < y_{J/\psi} < 4.5$) is applied to events saturating this distribution to compare with the first LHCb data [15].

Cutoff $2 < y_{J/\psi} < 4.5$ applied to the $pp \to J/\psi\psi' + X$, $\psi' \to J/\psi\pi\pi$ events simulated in Pythia generator selects approximately 16% of the total feed down cross section, which equals approximately 5.7 nb. This corresponds to the feed down in LHCb equal to

$$\sigma_{\text{LHCb}}^{\psi' \to J/\psi\pi\pi} (pp \to J/\psi\psi' + X) = 1.0\,\text{nb}.$$

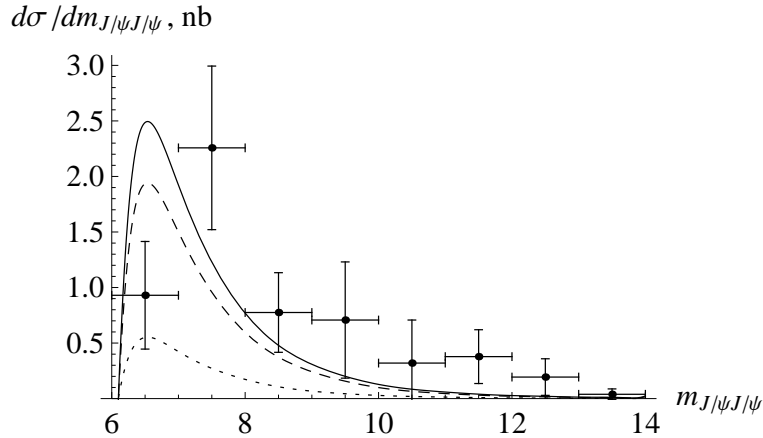FIG. 9. Distribution over the invariant mass of J/ψ pairs produced directly (dashed curve), with one J/ψ originated from ψ' decay (dotted curve) and their total (solid curve). LHCb kinematical cutoff is applied. Points with error bars correspond to the first LHCb data [15].

Together with the direct cross section this leads to the value

$$\sigma_{\text{LHCb}}^{total}\,(pp \to 2J/\psi + X) = 4.1 \pm 1.2\,\text{nb}.$$

Experimental value reported in [15] is 5.6 ± 1.1nb, which is in a good agreement with the prediction.

We make predictions for different kinematical distributions which will be measured by LHCb later at bigger statistics. Figures 10 and 11 show distributions over transverse momentum of a single J/ψ from a pair and over transverse momentum of the whole pair respectively. Contributions from both direct production and from ψ' decays are shown. One sees that shape of both contributions are similar. Fig. 12 shows distribution over the rapidity of one of the J/ψ mesons from a pair. Smooth left border of this distribution dues to the fact that two J/ψ mesons in a pair are generally close in rapidity. So when one of them fails cutoff in rapidity, second one is rejected too, even if it is in the allowed range.

IV.   TETRA-C-QUARK

The most interesting phenomenon in the region of small invariant masses of J/ψ-pairs is formation of a tetraquark built of 2 c-quarks and 2 $\bar{c}$-quarks and its decay into a J/ψ-pair. Similar states, for example exotic mesons $X(3872)$, $X(3940)$, $Y(3940)$ and $Y(4140)$, have already been observed in B-meson decays and $J/\psi\phi$, $J/\psi\omega$ invariant mass spectrums
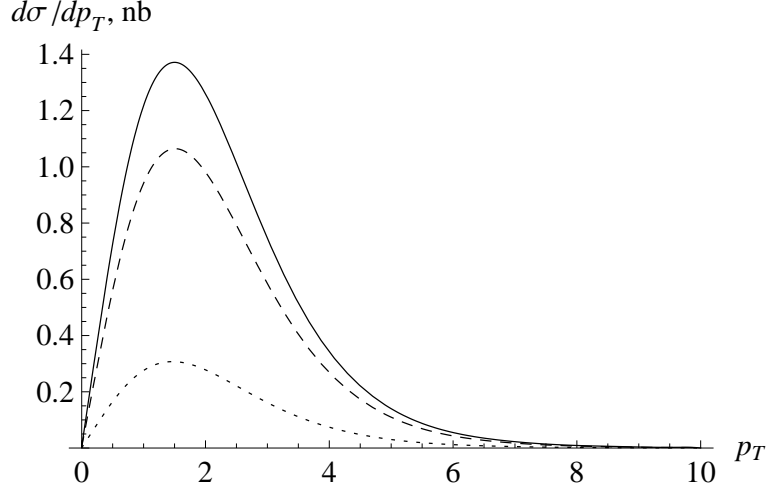
FIG. 10. Distribution over the transverse momentum of a single J/ψ-meson from the pair produced directly (dashed curve), with one J/ψ originated from ψ' decay (dotted curve) and their total (solid curve). LHCb kinematical cutoff is applied.
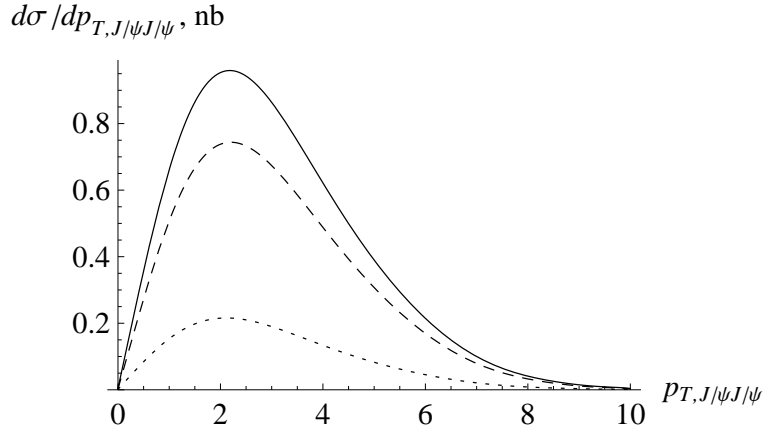

FIG. 11. Distribution over the transverse momentum of a J/ψ-meson pair produced directly (dashed curve), with one J/ψ originated from ψ' decay (dotted curve) and their total (solid curve). LHCb kinematical cutoff is applied.

[10, 11]. These states have small widths and can not be described in usual quark-antiquark scheme. It turns out, however, that all these mesons can be described in terms of tetraquarks $[cq]_{\bar{3}}\,[\bar{c}\bar{q}]_3$, where q is u-, d- or s-quark [8, 9]. In the following we consider the $q = c$ case, that is a tetraquark T_{4c} built from four charm quarks — $[cc][\bar{c}\bar{c}]$.

To estimate parameters of these states we use diquark model of tetraquark that is we assume that it is built from two almost point-like diquarks which interact with each other. In this case Pauli exclusion principle imposes strong restrictions on the quantum numbers
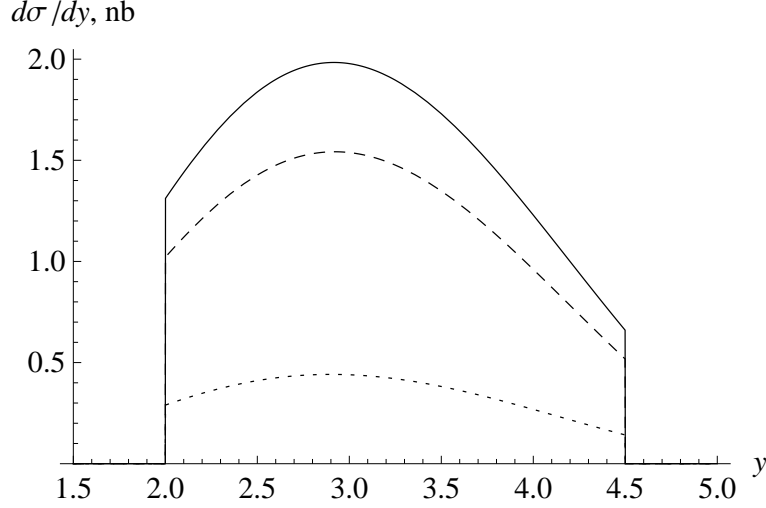
FIG. 12. Distribution over the rapidity of a single J/ψ-meson of the pair produced directly (dashed curve), with one J/ψ originated from ψ' decay (dotted curve) and their total (solid curve). LHCb kinematical cutoff is applied.

of these diquarks. Indeed, the angular momentum of quarks in the ground state of the diquark should be equal to zero. In order to attract to each other and build a tetraquark state both diquark and antidiquark should be in the triplet color state. From the Pauli exclusion principle it immediately follows that the total spin of both diquarks must be equal to unity. Indeed coordinate component of wave function of these diquarks is symmetric, color component — antisymmetric, so spin component of wave function has to be symmetric. Mass of a diquark with such quantum numbers can be determined by solving a non-relativistic Schrodinger equation [20, 23]. Interaction potential is chosen proportional to the potential between quark and antiquark in usual charmonium states but with an additional factor $1/2$ which accounts for the difference in color structures. Using mass of the c-quark equal to $m_c = 1.468$ GeV and taking into account hyperfine splitting

$$\Delta m = \frac{16\pi\alpha_s}{9m_c^2}(\mathbf{S_{c1}}\mathbf{S_{c2}})\left|\psi_{[cc]}(0)\right|^2 \sim 6.4\,\text{MeV},$$

where $\mathbf{S_{c1,2}}$ are quark spin operators and $\psi_{[cc]}(0)$ is the diquark wave function at origin, which value was given in expression (6), the following values for diquark mass and mean radius can be obtained:

$$m_{[cc]} = 3.13\,\text{GeV}, \qquad \left\langle r_{[cc]}\right\rangle = 0.523\,\text{fm}.$$

The following consideration assumes that both diquarks are point-like. In this case

tetraquark mass can be obtained by solving Schrodinger equation with the potential used in meson spectrum calculation. The wave function of tetraquark at origin appears to be equal

$$\psi_{T_{4c}}(r)|_{r=0} = 0.47\,\text{GeV}^{3/2}. \tag{8}$$

Without spin-spin interaction mass and mean radius of tetraquark are equal

$$M_{T_{4c}} = 6.12\,\text{GeV}, \qquad \langle r_{T_{4c}} \rangle = 0.29\,\text{fm}. \tag{9}$$

It is seen that the mean radius of tetraquark and its constituent diquarks are comparable, and therefore the values obtained for the masses should be regarded as a rough estimation. Finite size of the diquarks can be accounted for with the form factor

$$F\left(r^2\right) = \exp\left\{ -\frac{r^2}{\langle r_{[cc]}\rangle^2} \right\}.$$

Our calculations however show that this correction increases diquark mass only slightly, approximately by 40 MeV. Due to the spin-spin interaction, described by the potential

$$V_{SS}(r) = \frac{32\pi}{9} \frac{\alpha_s}{m_{[cc]}^2} (\mathbf{S_1 S_2})\delta(\mathbf{r}).$$

the state with mass (9) splits into scalar, axial and tensor tetraquarks with masses

$$J = 0: \qquad M_{T_{4c}(0^{++})} = 5.97\,\text{GeV},$$
$$J = 1: \qquad M_{T_{4c}(1^{+-})} = 6.05\,\text{GeV},$$
$$J = 2: \qquad M_{T_{4c}(2^{++})} = 6.22\,\text{GeV}.$$

It is evident that only tensor meson from this list is above the threshold of J/ψ-meson pair production. Corrections caused by the finite size of diquarks can, in principle, slightly increase masses and move the axial meson above this threshold, but its production in two gluon channel is forbidden by the charge parity conservation. As for the scalar tetraquark its decay into two real J/ψ mesons is kinematically forbidden. One of the final J/ψ-mesons, however, could be a virtual particle decaying into $\mu^+\mu^-$-pair. For this reason it is very interesting to search for the resonance in $J/\psi\mu^+\mu^-$ channel.

Duality relations can be used to estimate cross section of tetraquark production. Let us consider reaction $gg \to [cc]_{\bar{3}} + [\bar{c}\bar{c}]_3$ which cross section as a function of invariant mass of the system is plotted in fig.4. Below the threshold of 2 doubly-heavy baryons Ξ_{cc} diquarks
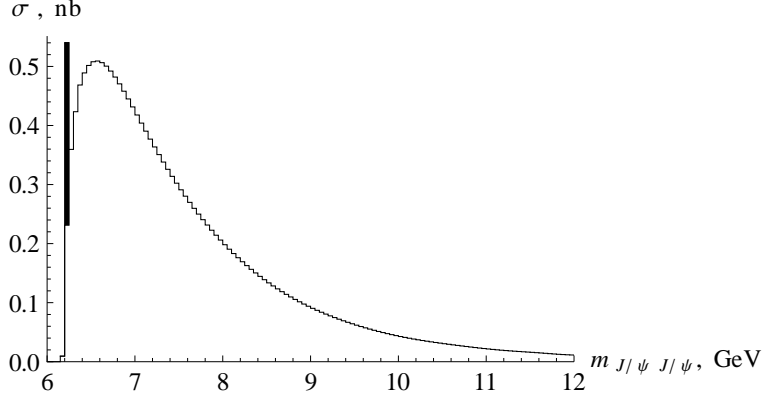
FIG. 13. Tetraquark contribution to the distribution over the invariant mass of the J/ψ-pair at 7TeV centre of mass energy.

can form a tetraquark T_{4c} consisting of 4 c-quarks with subsequent decay into a J/ψ meson pair. So, the following relation should hold:

$$S = \int_{2M_{J/\psi}}^{2M_{\Xi_{cc}}} dm_{gg}\sigma(gg \to X_{4c} \to 2J/\psi)$$

$$= K \cdot \int_{2M_{J/\psi}}^{2M_{\Xi_{cc}}} dm_{gg}\hat{\sigma}(gg \to [cc]_{\bar{3}} + [\bar{c}\bar{c}]_3) \approx K \cdot 6.4\,\mathrm{pb} \cdot \mathrm{GeV}, \quad (10)$$

where $K < 1$.

In the current work we use value $K = 0.1$. Width and height of the peak caused by the tetraquark contribution is determined by its own width $\Delta \sim 0.1$ MeV. However it is considerably smaller than experimental resolution of the detector $\Delta_{\mathrm{exp.}} \sim 50$ MeV. Histogram in Fig. 13 shows the distribution over the invariant mass of the J/ψ-pair with expected contribution from the tetraquark using experimental resolution for the bin width.

V. CONCLUSION

In our paper we use perturbative QCD to calculate the fourth order contributions to the J/ψ pairs production at LHC. According to our estimates the ratio of the cross section of this reaction to the cross section of single J/ψ-meson production in conditions of the LHCb experiment $(2 < y < 4.5)$ is about 4×10^{-4}. It should be noted, that comparison of the first experimental results at low energies with theoretical predictions shown excess of

experimental data by a factor $2 - 3$ [3]. Cross section predicted in our study is in a much better agreement with the recent LHCb result. Meanwhile all contributions accounted for in our work lead to kinematical peak corresponding to the first bin in experimental data presented. Possible contributions from the diquark-antidiquark production also lay in this invariant mass interval. If further experimental analysis eliminates lack of signal in the first bin preserving shape of the distribution corresponding increase of the cross section measured can amount to $50\% - 100\%$.

It is well known, that production and subsequent radiative decays of P-wave states χ_c can give additional contribution to J/ψ-meson cross section. Our estimates in the region of low invariant masses of the J/ψ pairs do not support this view, though it requires additional quantitative validation. Contribution form χ_c states can however become significant at large invariant masses and it is important to distinguish it from the color-octet one. The latter also is hardly noticeable in the kinematical region considered in our article. Other possible source of enhancement is inclusive production of J/ψ-pairs accompanied by additional gluons. Despite the fact that this process is described in the higher orders of perturbation theory, the number of color degrees of freedom in the final state increases greatly. It does not seem to be possible to distinguish experimentally exclusive J/ψ-pair production and reactions with emission of additional gluons. One can only estimate possible enhancement caused by contributions from higher orders of QCD. Thus accurate measurement of the cross section of double J/ψ production is needed.

Another interesting question considered is the possibility of observation of a new exotic meson built from 2 c-quarks and 2 $\bar{c}$-quarks. Our estimates show that if diquarks $[cc]$ and $[\bar{c}\bar{c}]$ are both in color-triplet states than in addition to attraction of quarks in diquark mutual attraction of diquarks exist. Rough estimation of masses of resulting tetraquarks is presented in our paper and in is shown that at least one of these states (tensor tetraquark) can be observed in $J/\psi J/\psi$ or $J/\psi \mu^+\mu^-$ modes.

[1] J. Badier *et al.* [NA3 Collaboration], Phys. Lett. **B114**, 457 (1982).

[2] J. Badier *et al.* [NA3 Collaboration], Phys. Lett. **B158**, 85 (1985).

[3] V. G. Kartvelishvili, S. .M. Esakiya, Sov.J.Nucl.Phys. **38**, 430-432 (1983).

[4] B. Humpert, P. Mery, Z. Phys. **C20**, 83 (1983).

[5] V. V. Kiselev, A. K. Likhoded, S. R. Slabospitsky, A. V. Tkabladze, Sov. J. Nucl. Phys. **49**, 682-687 (1989).

[6] C. -F. Qiao, L. -P. Sun, P. Sun, J. Phys. G **G37**, 075019 (2010). [arXiv:0903.0954 [hep-ph]].

[7] P. Ko, C. Yu, J. Lee, JHEP **1101**, 070 (2011). [arXiv:1007.3095 [hep-ph]].

[8] N. Drenska, R. Faccini, F. Piccinini, A. Polosa, F. Renga, C. Sabelli, Riv. Nuovo Cim. **033**, 633-712 (2010). [arXiv:1006.2741 [hep-ph]].

[9] S. S. Gershtein, A. K. Likhoded, G. P. Pronko, , [arXiv:0709.2058 [hep-ph]].

[10] F. Wick [On behalf of the CDF Collaboration], PoS **EPS-HEP2009**, 085 (2009). [arXiv:1011.0616 [hep-ex]].

[11] X. Liu, Z. -G. Luo, S. -L. Zhu, Phys. Lett. **B699**, 341-344 (2011). [arXiv:1011.1045 [hep-ph]].

[12] V. V. Braguta, A. K. Likhoded, A. V. Luchinsky, Phys. Rev. **D72**, 094018 (2005). [hep-ph/0506009].

[13] V. G. Kartvelishvili, A. K. Likhoded, Yad. Fiz. **40**, 1273 (1984).

[14] F. Maltoni, A. D. Polosa, Phys. Rev. **D70**, 054014 (2004). [hep-ph/0405082].

[15] CERN-LHCb-CONF-2011-009

[16] R. Mertig, M. Bohm, A. Denner, Comput. Phys. Commun. **64**, 345-359 (1991).

[17] A. V. Berezhnoy, V. V. Kiselev, A. K. Likhoded and A. I. Onishchenko, Phys. Rev. D **57**, 4385 (1998) [arXiv:hep-ph/9710339].

[18] A. V. Berezhnoy, V. V. Kiselev, A. K. Likhoded, Z. Phys. **A356**, 79-87 (1996). [hep-ph/9602347].

[19] R. Li, Y. -J. Zhang, K. -T. Chao, Phys. Rev. **D80**, 014020 (2009). [arXiv:0903.2250 [hep-ph]].

[20] V. V. Kiselev, A. K. Likhoded, O. N. Pakhomova, V. A. Saleev, Phys. Rev. **D66**, 034030 (2002). [hep-ph/0206140].

[21] T. Sjostrand, S. Mrenna and P. Z. Skands, JHEP **0605**, 026 (2006) [arXiv:hep-ph/0603175].

[22] J. Pumplin, D. R. Stump, J. Huston, H. L. Lai, P. M. Nadolsky and W. K. Tung, JHEP **0207**, 012 (2002) [arXiv:hep-ph/0201195].

[23] S. S. Gershtein, V. V. Kiselev, A. K. Likhoded, A. I. Onishchenko, , Phys. Rev. **D62**, 054021 (2000).